levels predicted by the theoretical relation, we have extracted data from [10] sufficient to compute the AE generated in the primary deformation zone per the first term of (1). For this purpose, Zorev's data for machining plain medium-carbon steel (40 steel) with nominal rake of ten degrees was used. For given speed and feed, cutting ratio r_c and average actual rake angle α_a were scaled from the experimental curves and used to compute shear angle as

$$\phi = \arctan \frac{\cos \alpha_a}{r_c - \sin \alpha_a} \tag{2}$$

Then a measure of the predicted acoustic emission in the primary zone was computed as

$$\text{RMS} = K \sin \alpha_a \left[U b_1 t_1 \frac{\cos \alpha_a}{\sin\phi \cos(\phi - \alpha_a)} \right]^{1/2} \tag{3}$$

where $K = C_4 \tau_k^{1/2}$ has been taken as constant.

Figure 8 shows the RMS computed in this manner as a function of cutting speed for three different values of feed. It is apparent that a portion of the curve for each feed exhibits an essentially linear, monotonically increasing character. However, we also observe a deviation from linear response for each feed when cutting speed is in the range for which a built-up edge is developed. For a feed of 0.195 mm, the deviation begins when cutting speed drops below approximately 100m/min while for the higher feeds this occurs at progressively lower speeds. The cutting speeds at which the built-up edge ceases to affect the acoustic emission at each feed correspond very closely to the conditions which provide a mean tool-chip contact temperature of around 600C in Zorev's experiments. That this is the temperature above which a BUE ceases to exist when machining steels is generally agreed [11].

Referring again to the data in Fig. 3 showing the mean acoustic emission RMS versus cutting speed for machining 4140 in our experiments, we note its similarity to the lower curve of computed data in Fig. 8. That the deviation from a linear relationship occurs at the higher speed of about 137 m/min is to be expected in light of the argument above since the feed is reduced relative to those of Fig. 8.

Summary

While it is difficult, if not impossible, to isolate a single effect in an oblique cutting operation, our experimental results provide strong evidence of a link between presence of a built-up edge and increased acoustic emission activity. We have hypothesized that the primary reason for this link is the increase in effective rake angle associated with the existence of a BUE. Calculated results using published experimental data in an existing theoretical relation appear to support the hypothesis. While the theoretical equation was developed for orthogonal cutting, it is nevertheless reasonable to apply it here to qualitatively examine our explanation of the experimental results. Finally, we note that our use of equation (3) ignores acoustic emission in the secondary and tertiary zones. The existence of a BUE would generally increase AE energy from these sources, so their inclusion should further support the experimental evidence presented here.

Further investigations are needed in order to better understand the BUE and acoustic emission relationship. It is planned to explore a wider range of workpiece materials, rake angle variations, and feeds. In future cutting experiments, comprehensive cutting force data will be obtained for correlation with AE measurements and BUE observations. Ultimately, it may be necessary to employ a quick-stop mechanism to quantify the built-up edge versus cutting conditions for inclusion in a process model.

References

1 Iwata, K., and Moriwaki, T., "An Application of Acoustic Emission Monitoring to In-Process Sensing of Tool Wear," *Annals of the CIRP*, Vol. 26, No. 1, 1977, pp. 21–26.

2 Dornfeld, D. A., and Kannatey-Asibu, E., "Acoustic Emission During Orthogonal Metal Cutting," *International Journal of Mechanical Science*, Vol. 22, No. 5, 1980, pp. 285–296.

3 Kannatey-Asibu, E., and Dornfeld, D. A., "Quantitative Relationships for Acoustic Emission from Orthogonal Metal Cutting," ASME JOURNAL OF ENGINEERING FOR INDUSTRY, Vol. 103, 1981, pp. 330–340.

4 Kannatey-Asibu, E., and Dornfeld, D. A., "A Study of Tool Wear Using Statistical Analysis of Metal Cutting Acoustic Emission," *Wear*, Vol. 76, No. 2, 1982, pp. 247–261.

5 Moriwaki, T., "Detection for Cutting Tool Fracture by Acoustic Emission Measurement," *Annals of the CIRP*, Vol. 29, No. 1, 1980, pp. 35–40.

6 Diei, E. N., and Dornfeld, D. A., "Acoustic Emission Sensing of Tool Wear in Face Milling," ASME JOURNAL OF ENGINEERING FOR INDUSTRY, Vol. 109, No. 3, 1987, pp. 234–240.

7 Yu, Q., and Hutton, D. V., "Liquid Coupled Acoustic Emission Measurement for Milling Operations," *Proceedings of the 16th North American Manufacturing Research Conference*, University of Illinois, 1988, pp. 403–407.

8 Shaw, M. C., Cook, N. H., and Smith, P. A., "The Mechanics of Three Dimensional Metal Cutting," *Transactions of the ASME*, Vol. 74, No. 6, 1952, pp. 1055–1064.

9 Lee, E. H., and Shaffer, B. W., "The Theory of Plasticity Applied to a Problem of Machining," ASME *Journal of Applied Mechanics*, Vol. 73, 1954, pp. 405–413.

10 Zorev, N. N., *Metal Cutting Mechanics*, Pergamon Press, 1965, Chap. 4.

11 Shaw, Milton C., *Metal Cutting Principles*, Clarendon Press, Oxford, 1984, pp. 501–509.

Effects of Geometric and Process Parameters on Drill Transverse Vibrations

O. Tekinalp[1] and A. Galip Ulsoy[2]

Finite element solutions are used to analyze the effects of geometric and process parameters on the drill bit transverse vibrations. The effects of cross sectional geometry, of the flute helix angle, the drill rotational speed, and the thrust force generated during drilling on the drill transverse frequencies are investigated. Simulation results also show the transient vibrations of a drill bit under transverse cutting forces at the drill tip.

Introduction

Drilling is economically one of the most important manufacturing operations [1], and drill structural properties have a direct bearing on the performance of the drilling process. The vibration signal generated during drilling may be used for drill wear and breakage detection [2–5]. Drill bit stability becomes important when drilling small holes or drilling at high speeds [6–8]. The importance of drill bit vibrations on hole quality has also been emphasized by numerous authors [9–11]. Hole quality in turn is important for the performance of the manufactured part. For example, in the aircraft industry, defective fastener holes are known to promote fatigue, and result in catastrophic failure of aircraft wings or other structural elements [12–13]. Hence, various researchers have concentrated on modeling the dynamic behavior of drill bits [14–18].

The early research in drilling concentrated on the investigation of drilling as an orthogonal cutting process [19–20].

[1]Graduate Student and Student Member, ASME

[2]Associate Professor and Member, ASME, Department of Mechanical Engineering and Applied Mechanics, The University of Michigan, Ann Arbor, MI 48109-2125.

Contributed by the Production Engineering Division for publication in the Journal of Engineering for Industry. Manuscript received October 20, 1988; revised July 19, 1989.

The torque and thrust generated in drilling, and the effect of drill point geometry on these forces has been investigated extensively [21–23]. Characterizing the effect of drill point geometry on tool life, and designing better drill points has been one of the primary goals in drilling [24]. Researchers have also concentrated on modeling complex drill point geometries [25–27].

This paper is a continuation of the work previously reported in [15–18]. The experimentally validated distributed parameter model, and the associated finite element solution method, described in [18] is used here to investigate the effect of various geometric and operational parameters on the drill bit performance. The effect of the cutting process in drilling is only indirectly considered through the externally applied forces. The parameters considered here are: drill cross sectional geometry, drill flute helix angle, drill rotational speed, and thrust force.

Modeling

The model and solution method used to obtain the results presented here has been described in detail in a previous paper [18]. The model developed was validated by first comparing the finite element solutions to some known analytical solutions from the literature [18]. The finite element results were then also compared to the experimental results reported in [16, 17]. Good agreement was observed between experimental and theoretical transverse natural frequencies when using a clamped-pinned boundary condition in the finite element solutions. In certain cases the solutions were closer to the clamped-clamped boundary condition solutions due to the amplitude dependent nature of the vibrations in the experiments. That is, at small amplitudes the drill bit behaved like a beam clamped at the chuck and pinned at the hole bottom, whereas at high excitation amplitudes it behaved like a beam clamped at the chuck and clamped at the hole edge. The computer program used to generate the results in the next section is described in [28], which also contains the program listings.

One part of the computer program calculates drill bit cross sectional properties. First the user inputs the coordinates of certain points obtained from measurements on a drill cross section. For analysis purposes the drill cross section is approximated using 4 curves connecting 5 points along the boundary (see Fig. 1). The program then automatically generates the boundary mesh and the corresponding triangular interior mesh. The mesh generated is used to calculate the cross sectional area and the principal area moments of inertia of the drill bit.

The model developed includes the thrust (axial) force, transverse cutting forces and torque, rotation of the drill bit, drill helix angle, and drill cross sectional properties. Thus, it includes the important structural and operational parameters of drill bits. Together with the solution method developed, the model is potentially useful for drill bit sensitivity, optimization, and control studies. Some parametric studies are presented in the next section in terms of the drill transverse natural frequencies. It can be conjectured that high natural frequencies will result in a high dynamic stiffness, and consequently good drilled hole quality. However, quantitative studies relating drill natural frequency spectra to drilling performance have not been reported.

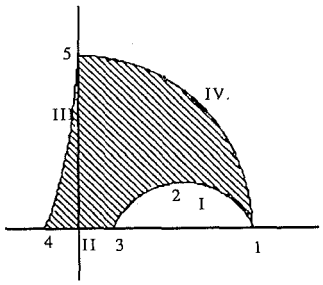

Fig. 1 Drill cross sectional geometry used for mesh generation. Due to symmetry only the upper half of the cross section is shown.

Results and Discussion

Drill bit bending frequencies depend upon both process parameters, and geometric parameters. Process parameters considered here are the rotational speed and feedrate. Geometric parameters are the drill length, drill flute helix angle, drill cross sectional area, cross sectional area moments of inertias, and drill point geometry. Considered here are the drill cross sectional geometry, and the drill flute helix angle. For sensitivity studies in terms of these parameters a nominal drill with diameter $D = 9.525$ mm is used at two different lengths, $l = 0.1$ m and, $l = 0.2$ m. All finite element solutions are obtained for clamped-pinned boundary conditions. Since rotating shafts with dissimilar moments of inertia have different frequencies for forward and reverse precession [29], both frequencies are shown in Figs. 4–11. The frequencies are normalized by dividing them by the lowest forward precession speed of the nominal drills. For easy reference the nominal cases are indicated by a vertical line in each plot. The assumed nominal values are as follows: nominal thrust force, $F_z = 1730$ kN; nominal rotational speed, $\omega_0 = 10$ Hz; nominal helix angle for the short drill ($l = 0.1$ m) is $\beta_0 = 94$ rad/m, and the nominal helix angle for the long drill ($l = 0.2$ m) is $\beta_0 = 47$ rad/m.

Cross Sectional Geometry. Figure 2 shows the cross section of the $D = 9.525$ mm drill bit used in the experiments reported in [17]. Drill cross sectional parameters are calculated for this cross section for the $D = 9.525$ mm drill bit and for the $D = 6.35$ mm drill. The results are given in Table 1 together with the corresponding cross sectional properties of solid shafts of the same diameter. It can be observed that the drill cross sectional area is approximately half of the cross sectional area of the solid shaft. The area moments of inertias are 65–70 percent of the solid one in one principal direction, and 13–15

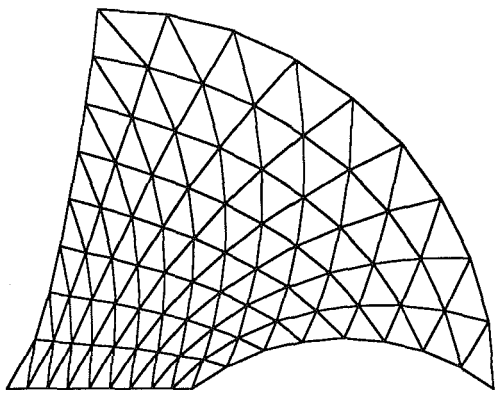

Fig. 2 Triangular mesh generated for $D = 9.525$ mm nominal drill cross section using automatic mesh generation routines. $I_1 = 58.61\ 10^{-12}$ m^4, $I_2 = 290.2\ 10^{-12}$ m^4, Area $= 34.59\ 10^{-6}$ m^2

Table 1 Cross sectional properties of two twist drills used in [17], and also the cross sectional properties of solid shafts of the same diameter

	$D = 6.25$ mm		$D = 9.535$ mm	
	drill	shaft	drill	shaft
I_1 (m^4)	5.24E-11	7.98E-11	2.90E-10	4.04E-10
I_2 (m^4)	9.77E-12		5.86E-11	
Area (m^2)	1.37E-05	3.17E-05	3.46E-05	7.13E-05

Table 2 Comparison of the bending frequencies of the D = 9.525 mm nominal drill and the thick web drill. Forward and reverse first bending frequencies in two orthogonal directions are given for: l = 0.2 m, β_0 = 47 rad/m, F_z = 1.73 kN, ω_0 = 10 Hz

	Nominal drill (Hz)	Thick web drill (Hz)
ω^f_{nx}	467	447
ω^r_{nx}	-447	-437
ω^f_{ny}	1550	1477
ω^r_{ny}	-1530	-1457

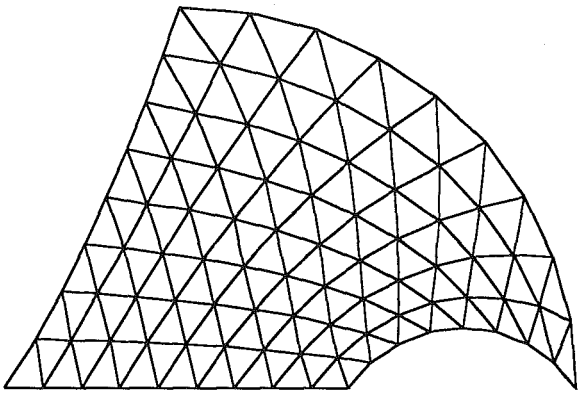

Fig. 3 The new cross section obtained by doubling the web thickness of the standard D = 9.525 mm drill. I_1 = 61.43 10^{-12} m^4, I_2 = 303.59 10^{-12} m^4, Area = 39.41 10^{-6} m^2

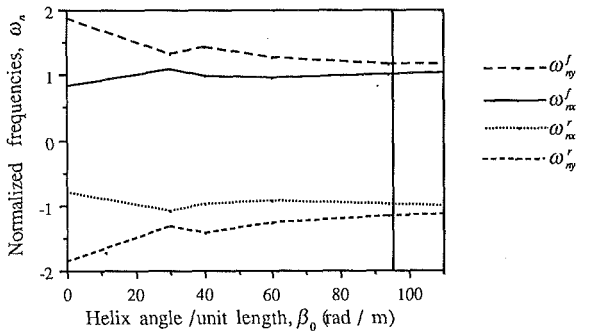

Fig. 4 Change in natural frequencies with helix angle (40 elements). D = 9.525 mm, l = 0.1 m, ω_0 = 10 Hz, F_z = 1.73 kN

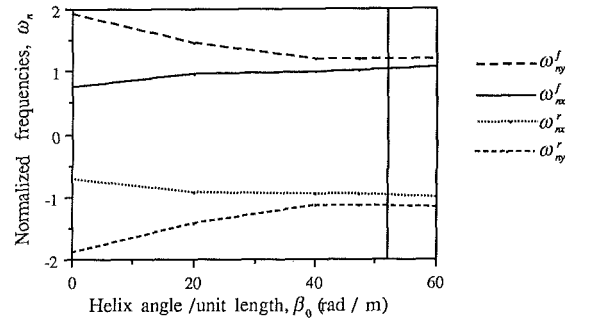

Fig. 5 Change in natural frequencies with helix angle (40 elements). D = 9.525 mm, l = 0.2 m, ω_0 = 10 Hz, F_z = 1.73 kN

percent of the solid one in the other principal direction. Burnham [7] suggests that one can use an equivalent diameter to calculate the bending stiffness of a drill and recommends the formula,

$$D_e = 0.788\ D \tag{1}$$

How can we, for example, change the cross sectional geometry to increase the bending stiffness of a drill cross section? Moreover, how will this change in the cross sectional geometry effect the bending frequencies of drill bits? To analyze these cross sectional effects, the cross section of the nominal drill (D = 9.525 mm, shown in Fig. 2) is changed by doubling its web thickness (i.e., the line II in Fig. 1). The new cross section is given in Fig. 3. The cross sectional area and area moments of inertias are also given in the captions of Figs. 2 and 3. Increasing the web thickness increases both the cross sectional area moments of inertia and the cross sectional area. The bending frequencies for this new cross section and for the nominal cross section are given in Table 2. There is only a slight drop in the bending frequencies with this new cross section, which is due to the substantial increase in cross sectional area compared to the cross sectional area moment of inertias. Hence the new cross section has not affected the bending stiffness or bending frequencies substantially. Here a change in the web thickness is considered for illustrative purposes only, one cannot change the drill cross section arbitrarily. The basic shape and its effect on the drill point should be considered. Although not presented here, other possible changes in the drill cross sectional geometry were also analyzed. The gain in bending stiffness or bending frequencies was typically negligible.

Drill Helix Angle. The helix angle, β_0, is one of the most important structural properties of drill bits, and its effect on the bending frequencies is shown in Figs. 4 and 5. The untwisted short drill has a fundamental bending frequency of ω^f_{nx} = 1599 Hz (forward precession) with increasing twist this frequency increases to 1971 Hz when β_0 = 94 rad/m. Hence there is almost a 23 percent increase in the fundamental bending frequency. As can be seen from the graphs the first bending frequencies in the two principal directions get closer and closer and tend toward an average value. That is, an increase in β_0 increases the bending stiffness. Note that the nominal helix angle selected for each of the drills corresponds to a total of 1.5 turns along the drill length. In the manufacturing of drill bits the amount of twist is determined according to certain cutting properties. Too much twist may result in the entanglement of chips in the drill helix groove and make cutting difficult due to increased friction and rubbing. On the other hand as can be seen from Figs. 4 and 5 the amount of twist affects the bending stiffness of the drill bit. However, there is a region above 80 rad/m for the short drill and 40 rad/m for the long drill where change in the fundamental natural frequency is less than 5 percent. Thus, for both drills, there is not much to be gained in terms of increased natural frequencies by introducing more than 1.5 turns along the drill length.

Drill Rotational Speed. In Figs. 6 and 7 the effect of spindle speed, ω_0, on the bending frequencies of short and long drills is illustrated. As the spindle speed increases both forward and reverse precession frequencies in two orthogonal directions increase. This effect, as shown in Fig. 8, becomes much more pronounced for slender drills. In this case the lower fundamental precession speeds for forward and reverse precession approach one another and become equal for a rotational speed around 65 Hz. At this frequency (65 Hz) the rotational speed (thick line) is equal to the precession speed, and the drill bit is unstable above this critical speed [29]. The rotational speed for a drill bit is selected with the cutting speed in mind. Like other cutting processes, in drilling the cutting speed is limited for a given tool workpiece interface. Higher cutting speeds result in poor tool life. In drilling the cutting speed varies along the drill lip, and the highest cutting speed is achieved at the drill periphery. Hence to keep the cutting speed optimal, lower

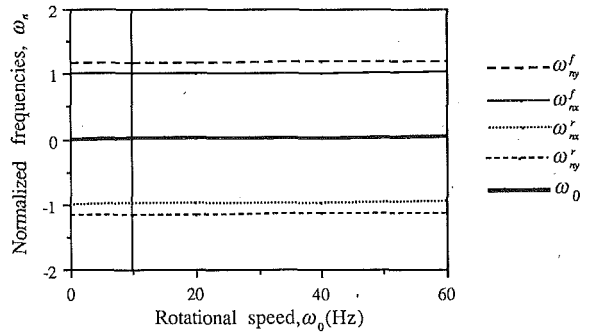

Fig. 6 Change in natural frequencies with rotational speed (40 elements). D = 9.525 mm, l = 0.1 mm, F_z = 1.73 kN, β_0 = 94 rad/m

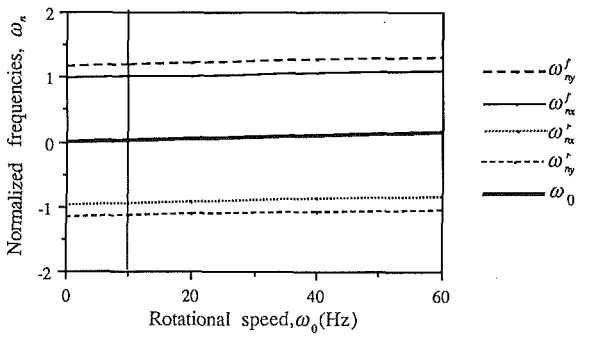

Fig. 7 Change in natural frequencies with rotational speed (40 elements). D = 9.525 mm, l = 0.2 m, F_z = 1.73 kN, β_0 = 47 rad/m

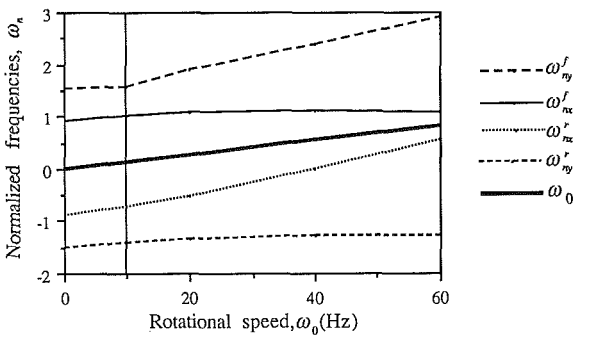

Fig. 8 Change in natural frequencies with rotational speed (40 elements). D = 6.35 mm, l = 0.24 m, F_z = 1.05 kN, β_0 = 47 rad/m

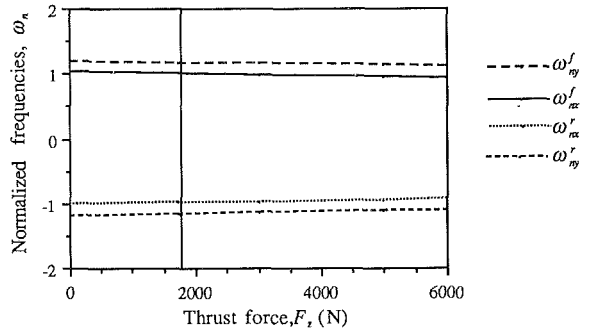

Fig. 9 Change in natural frequencies with thrust force (40 elements). D = 9.525 mm, l = 0.1 m, ω_0 = 10 Hz, β_0 = 94 rad/m

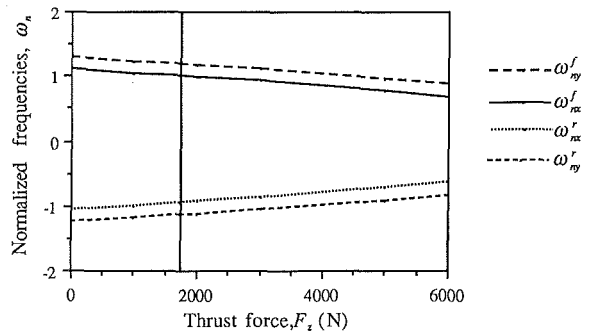

Fig. 10 Change in natural frequencies with thrust force (40 elements). D = 9.525 mm, l = 0.2 m, ω_0 = 10 Hz, β_0 = 47 rad/m

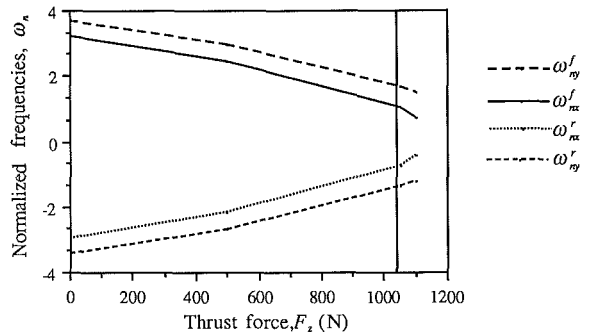

Fig. 11 Change in natural frequencies with thrust force (40 elements). D = 6.35 mm, l = 0.24 m, ω_0 = 10 Hz, β_0 = 47 rad/m

spindle speeds are used for larger diameter drills. On the other hand different workpiece materials may permit different cutting speeds. For example, a major tool manufacturer recommends a 10 Hz spindle speed when drilling a 1020 steel with a D = 9.525 mm drill. The recommended spindle speed is increased to 30 Hz when drilling aluminum, and to 35 Hz when drilling aluminum with a D = 6.35 mm drill. Twist drills are typically operated well below the critical speed region. However, as shown in Fig. 8, slender drills may become unstable at spindle speeds close to those used in normal operation. This phenomenon has been observed in previously reported experiments when drilling with long (l = 0.24 m), and slender (D = 3.175 mm, and D = 4.763 mm) drills [16].

Thrust Force. The effect of thrust force, F_z, on the natural frequencies is shown in Figs. 9–11. The nominal value of thrust, corresponding to recommended speeds and feeds, is again shown by the vertical line in each figure. As can be seen from these figures, increase in thrust force results in a decrease in the natural frequencies. The effect of thrust force on the bending frequencies of twist drills is much more pronounced in slender drills, as expected. The thrust force is a function of feedrate, drill point geometry, and the workpiece material. For example, a thrust force formula given by Shaw [21] is,

$$F_z = D^2 H_b \frac{C_1 f^{0.8}}{D^{1.2}} \times \left[\frac{1 - \frac{w}{D}}{\left(1 + \frac{w}{D}\right)^{0.2}} + 2.2 \left(\frac{w}{D}\right)^{0.8} \right] + C_2 \left(\frac{w}{D}\right)^2 \quad (2)$$

where, f is the feedrate, H_b the Brinell hardness of the workpiece, w the web thickness, D the drill diameter, and C_1 and C_2 are constants. For a given drill, thrust force increases with the feedrate. Feedrate affects the depth of cut, and the tool life. Hence, it is typically optimized with respect to tool life. However, for long and thin drills the feedrate is decided solely based on the buckling condition of the drill bit [6–7, 16]. In Fig. 11 bending frequencies for a slender drill are given (D = 6.35 mm, and l = 0.24 m). This drill will buckle beyond a thrust force of 1100 N. When the recommended feed [30] for a shorter size of this drill is used, the drill will be very close to the buckling point (vertical line). In practice the drill bit

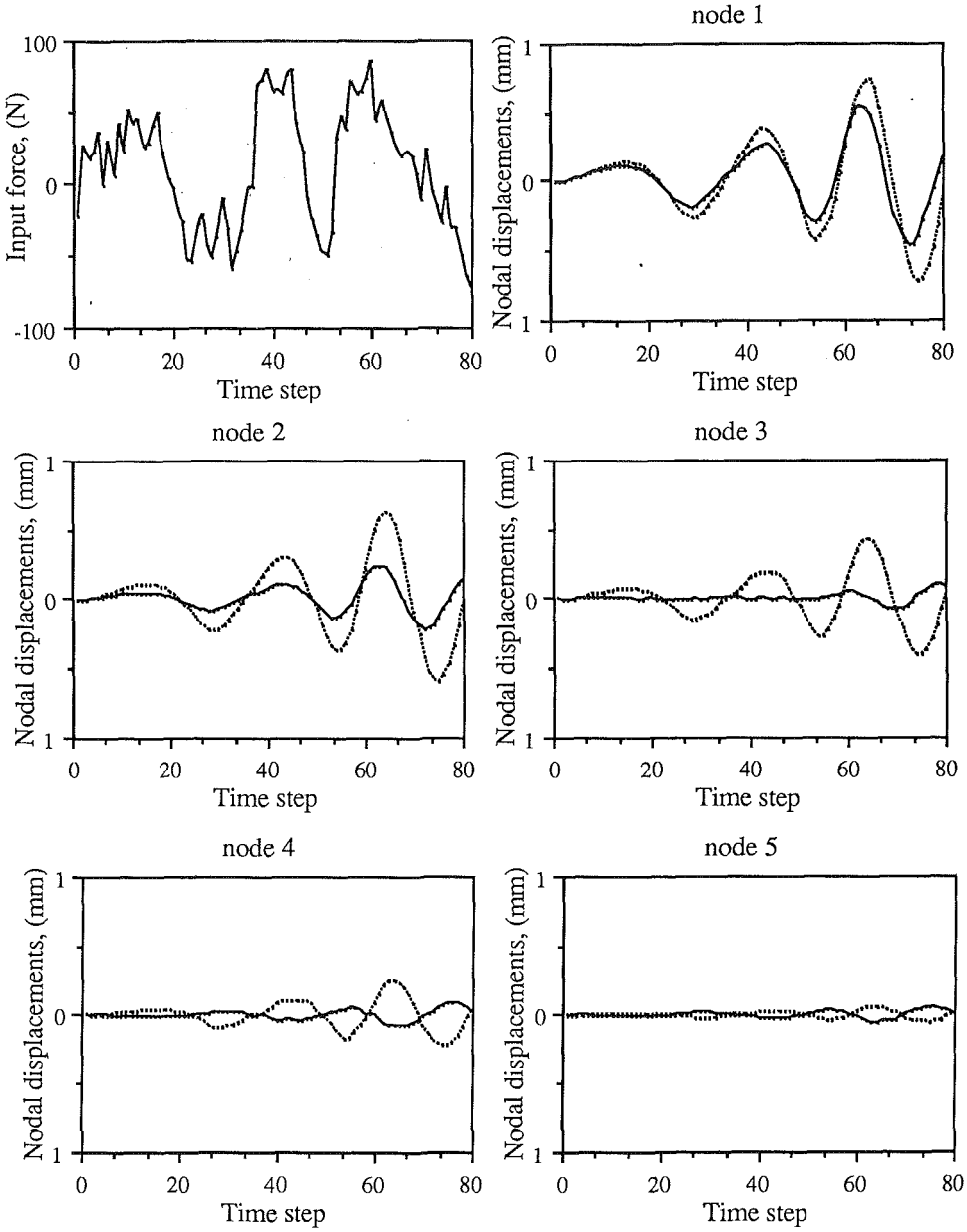

Fig. 12 Input force and corresponding time response at various nodes in two orthogonal directions (5 elements). D = 9.525 mm, l = 0.1 m, β_0 = 94 rad/m, F_z = 1.73 kN, ω_0 = 10 Hz, total time span = 0.003 s. = 80 time steps.

will buckle below this theoretical point since drill bits are not ideally straight.

Transverse Forces. To test the significance of the transverse cutting force components on drill bit vibrations a simulation is performed. The drill bits considered are subjected to a random transverse cutting force, well within the limits of transverse cutting forces typically measured while drilling. This random force is applied to the drill after lowpass filtering. Figure 12 shows the filtered input and deflection of the shorter (l = 0.1 m) drill bit at each of the 5 nodes in the finite element solution. This drill shows a 0.8 mm maximum deflection near the tip, which is rather large and certainly unacceptable for a drilling operation. It should be recognized, however, that a drilling operation starts with a center punch operation to get the drill going correctly into the material. For regular twist drills the drill bit will not feed into the material and wander around or simply break without a center punch. Once inside the hole the drill generally gets support from the walls of the hole and does not wander very much. However, for high precision drilling even a very small imperfection in the hole may be unacceptable [12, 13]. Similar results, although not shown here, were also obtained for the longer (l = 0.2 m) drill, and maximum vibration amplitudes in that case were observed to be as high as 6 mm.

Summary and Conclusions

The predictions of a previously presented and validated [18] model are used to show the importance of various parameters on drill bit performance. In particular the effects of rotational speed, thrust force, helix angle, and cross sectional properties are discussed. The rotational speed has a direct effect on the stability of the drill bits, but this effect is not significant for standard spindle speeds and short drills. However, when slender drills are used higher rotational speeds are shown to cause instability. Thrust force also becomes important for long slender drills. It is shown that for long slender drills of dimensions

readily available in the market, low feedrates should be used to prevent buckling. Helix angle affects drill bits by increasing the transverse stability of the drills. Typically an untwisted (β_0 = 0 rad/m) drill will have a minimum bending stiffness that is half that of a twisted one. It is shown that the contribution of the helix angle to the bending stiffness becomes negligible after approximately 1.5 turns along the length. The effect of cross sectional properties of twist drills on bending frequencies is also investigated. It is found that, while retaining the basic geometry of the drill cross section, not much improvement can be achieved.

The model of drill vibrations presented here is potentially useful for studies in drill design, process optimization, and process control. Although the model presented here is rather general, it may be desirable to incorporate some extensions to more complex drill geometries (e.g., multiple flutes). It is also desirable to combine this type of vibration model with a model of the cutting process in drilling (e.g., [31]). Such a combined cutting process and drill vibration model is an important topic for future research.

Acknowledgments

The authors would like to thank Dr. James MacBain for his valuable contributions to the development of the model, and to acknowledge the financial support of the Industrial Technology Institute and TRW Inc.

References

1 Khang, C. H., "Research Goals in High Speed Drilling," SME Paper No. MR77-384, 1977.

2 Braun, S., Lenz, E., and Wu, C. L., "Signature Analysis Applied to Drilling," ASME Paper No. 81-Det-9, 1981.

3 Yee, W. K., and Bloomquist, D. S., "On Line Method of Determining Tool Wear by Time Domain Analysis," SME Paper No. MR82-901, 1982.

4 Yee, K. W., "On Line Use of Drill-Up for On-Line Determination of Drill Wear," *SME Paper, No. MS84-914*, 1984.

5 Moore, T., and Reif, Z., "Using Vibration Data to Detect Drill Breakage in High Volume," *SME Paper No. MS84-908*, 1984.

6 Burnham, M. W., "An Analysis of Drill Deflection for Deep Miniature Holes," ASME Paper No. MR80-956, 1980.

7 Burnham, M. W., "The Mechanics of Drilling Small Holes," 10th North American Manufacturing Research Conference, Ontario, May 1983.

8 Wilson, A. J., "Failure of a Drill Near Critical Speed," ASME Paper No. 84-WA/DE-22, 1984.

9 Fuji, H., Marui, E., and Satsoki, E., "Whirling Vibration in Drilling, Part 1: Cause of Vibration and Role of Chisel Edge," ASME *Journal of Engineering for Industry*, Vol. 100, No. 3, August 1986.

10 Fuji, H., Marui, E., and Satoski, E., "Whirling Vibrations in Drilling, Part 2: Influence of Drill Geometry, Particularly of the Drill Flank on the Initiation of Vibration," ASME JOURNAL OF ENGINEERING FOR INDUSTRY, Vol. 100, No. 3, August 1986.

11 Reinhall, P. G., and Storti, D. W., "Modeling and Analysis of the Dynamics of a Drill Penetrating a Thin Plate," ASME Paper No. 86-WA-33, 1986.

12 Rudd, J. L., and Gray, T. D., "Quantification of Fastener-Hole Quality," *Journal of Aircraft*, Vol. 15, No. 3, March 1978, pp. 143–147.

13 Renshaw, T., Wongwiwat, K., and Sarrantonio, A., "Comparison of Properties of Joints Prepared by Ultrasonic Welding and Other Means," *Journal of Aircraft*, Vol. 20, No. 6, June 1983, pp. 552–556.

14 Magrab, E., and Glisin, D. E., "Buckling Loads and Natural Frequencies of Twist Drills," ASME Paper No. 84-WA/Prod-12, 1984.

15 Ulsoy, A. G., "A Lumped Parameter Model for the Transverse Vibration of Drill Bits," in Hardt, D. E., and Book, W. J., eds, *Control of Manufacturing Process and Robotic Systems*, ASME, 1983, pp. 15–25.

16 Ulsoy, A. G., and Tekinalp, O., "Dynamic Modeling of Transverse Drill Bit Vibrations," *Annals of the CIRP*, Vol. 33, No. 1, 1984, pp. 253–258.

17 MacBain, J. C., Harding, K. G., and Tekinalp, O., "Vibration Modes and Frequencies of Twist Drills Using Laser Holographic Interferometry," *Symposium on Sensors and Controls for Manufacturing*, ASME Winter Annual Meeting, November 17–22, 1985, Miami Beach, Florida.

18 Tekinalp, O., and Ulsoy, A. G., "Modeling and Finite Element Analysis of Drill Bit Vibrations," ASME *Journal of Vibration, Acoustics, Stress and Reliability in Design*, Vol. 111, No. 2, April 1989, pp. 148–155.

19 Galloway, D. F., "Some Experiments on the Influence of Various Factors on Drill Performance," ASME *Transactions*, Vol. 77, July 1957, pp. 191–230.

20 Oxford, C. J., Jr., "On the Drilling of Metals—I Basic Mechanics of the Process," *Transactions*, Vol. 77, Feb. 1955, pp. 103–114.

21 Shaw, M. C., and Oxford, C. J., Jr., "On the Drilling of Metals—II Torque and Thrust in Drilling," ASME *Transactions*, Vol. 79, January 1957.

22 Williams, R. A., "A Study of the Drilling Process," ASME *Journal of Engineering for Industry*, November 1974, pp. 1207–1215.

23 Oxford, C. J., "Review of Some Recent Developments in the Design and Application of Twist Drills," *Advances in Machine Tool Design and Research*, 1967, pp. 845–861.

24 Kaldor, S., and Lenz, E., "Drill Point Geometry and Optimization," ASME *Journal of Engineering for Industry*, Vol. 105, February 1982, pp. 173–182.

25 Fugelso, M. A., "Cylindrical Flank Twist Drill Points," ASME *Journal of Engineering for Industry*, Vol. 105, August 1970, pp. 183–186.

26 Wu, S. M., and Shen, J. M., "Mathematical Model for Multifacet Drills," ASME *Journal of Engineering for Industry*, August 1970.

27 Chen, L. H., and Wu, S. M., "Further Investigation of Multifacet Drills (MFD's)—Mathematical Models, Methods of Grinding, and Computer Plotting," ASME *Journal of Engineering for Industry*, Vol. 106, November, 1984, pp. 313–324.

28 Tekinalp, O., and Ulsoy, A. G., *Computer Programs Developed to Solve the Equations of Motion for Drill Dynamics*, Technical Report No. UM-MEAM-88-02, Department of Mechanical Engineering and Applied Mechanics, University of Michigan, Ann Arbor, Michigan, May 1988.

29 Dimentberg, F. M., *Flexural Vibrations of Rotating Shafts*, Butterworths, London, 1961.

30 Kronenberg, M., *Drilling Feeds*, Machinery, London, 1935.

31 Stevenson, D. A., and Wu, S. M., "Computer Models for the Mechanics of Three-Dimensional Cutting Processes, Part I: Theory and Numerical Method, Part II: Results for End Turning and Drilling," ASME *Journal of Engineering for Industry*, (accepted for publication).

Experimental Investigations into Electrochemical Spark Machining of Composites

V. K. Jain[1], S. Tandon[2], and P. Kumar[3]

Reports have indicated the poor performance of the conventional type of cutting tools during machining of composites. In this paper electrochemical spark machining (ECSM) for the cutting and drilling of holes in the composites is being proposed. The feasibility of using ECSM for composites was first ascertained. Then, kevlar-fiber-epoxy and glass-fiber-epoxy composites as work material, copper as tool material, and an aqueous solution of NaCl as electrolyte were used. It has been concluded that the ECSM is a viable solution for cutting of Fiber Reinforced Plastics (FRP). For achieving desired accuracy, surface finish, and economics of the process, the machining parameters should be optimized.

1 Introduction

The machining of composites requires special consideration about the wear resistance properties of the tool materials and the cutting tool geometry. High speed steel (HSS) is unsuitable as a tool material for machining composites because of its comparatively low wear resistance. Hence, carbides and diamonds are used as tool materials. A serious problem of FRP machining is the generation of airborne dust. The dust has to be extracted and filtered out carefully, otherwise serious health hazards may occur [1]. Drilling in composites [2, 3] results in delamination, and furry and undersized holes. Another major problem faced during drilling of FRP is the inconsistency in the quality achieved at the tool exit side [1]. Another method used for machining of FRP is water jet cutting (WJC) [4]. From a physical point of view, the water jet has good preconditions for cutting FRP as there is no potential for thermal

[1]Visiting Professor, Dept. of Mech. Engr., Univ. of California, Berkeley, CA 94720

[2]Graduate Student, Dept. of Mech. Eng., Indian Institute of Technology, Kanpur-208016, India

[3]Professor, Dept. of Mech. Eng., Indian Institute of Technology, Kanpur-208016, India

Contributed by the Production Engineering Division for publication in the JOURNAL OF ENGINEERING FOR INDUSTRY. Manuscript received January 17, 1988.